Energy & Environmental Science

Accepted Manuscript

Energy and Environmental Science RSCPublishing

Perspective

Oxygen tolerant proton reduction catalysis: Much O_2 about nothing

Cite this: DOI: 10.1039/x0xx00000x

Received 00th January 2012,
Accepted 00th January 2012

DOI: 10.1039/x0xx00000x

www.rsc.org/

David W. Wakerley[a] and Erwin Reisner*[a]

Proton reduction catalysts are an integral component of artificial photosynthetic systems for the production of H_2. This perspective covers such catalysts with respect to their tolerance towards the potential catalyst inhibitor O_2. O_2 is abundant in our atmosphere and generated as a by-product during the water splitting process, therefore maintaining proton reduction activity in the presence of O_2 is important for the widespread production of H_2. This perspective article summarises viable strategies for avoiding the adverse effects of aerobic environments to encourage their adoption and improvement in future research. H_2-evolving enzymatic systems, molecular synthetic catalysts and catalytic surfaces are discussed with respect to their interaction with O_2 and analytical techniques through which O_2-tolerant catalysts can be studied are described.

1. Introduction

The large scale production of H_2 through artificial photosynthesis stands as an aspiring goal of contemporary science.[1–3] Chemical-energy storage through water splitting generates both H_2 and O_2 and relies on efficient reduction and oxidation catalysts, respectively [reaction (1)].

$$H_2O \rightarrow H_2 + \tfrac{1}{2}O_2 \qquad \Delta E^o = 1.23\ \text{V} \qquad (1)$$

Research into viable catalysts is consequently gathering significant interest,[4] but there remain several limitations that must be addressed before such systems can be implemented on a commercial scale. For example, avoiding non-aqueous solutions, increasing long-term stability and sustaining high catalytic efficiency are all goals for a benchmark catalyst and progress in these areas has proceeded at an appreciable rate.

One issue that remains relatively underexplored is the impact of O_2 on synthetic proton-reducing systems. Less than a decade ago it seemed common sense that synthetic molecular H_2-evolving catalysts would operate poorly under air due to the propensity of O_2 to irreversibly damage a catalytic structure. As a result, research was carried out under inert atmospheres of N_2 or Ar. Given that the end goal for a proton reduction catalyst would be its widespread use in a H_2-fuelled economy, any observable O_2-sensitivity would seriously impair its practicality. Adding to this, stringent anaerobic conditions are costly to maintain on an industrial scale. Developing catalysts that could operate under O_2 consequently stood as a major challenge for H_2 production research,[5,6] yet recent publications have demonstrated that avoiding the inhibiting effects of O_2 may be more manageable than first imagined and O_2-tolerant proton reduction is now a fast-developing field.

Exposure of a proton reduction catalyst to O_2, particularly over prolonged periods of time, is almost unavoidable. Figure 1a shows a standard electrolyser/photoelectrochemical (PEC) cell, which contains an O_2 evolving anode and a H_2 producing cathode separated by a proton exchange membrane to prevent crossover of the evolved gaseous products.[7] Interaction between O_2 and the proton reducing cathode can still occur through O_2 leakage from the atmosphere into the electrochemical cell or from the anodic chamber after membrane degradation.[8,9] Another set up is the 'artificial leaf',[10,11] a simplification of which can be seen in Figure 1b. The cathode and anode are attached on opposing sides of a photovoltaic layer that drives catalysis and exposure of the proton reduction catalyst to O_2 is inherent in the system's design. Photocatalytic water-splitting particles are also a promising route to full water splitting, see Figure 1c.[12,13] H_2 and O_2 are produced on the same or a neighbouring light-absorbing particle, which is often loaded with a cocatalyst to enhance catalysis. The close proximity of O_2 and H_2 evolution sites makes interaction between catalyst and O_2 inevitable without additional protection of the catalyst.

Contemporary research has started to cover the concept of O_2-tolerant H_2 generation to realise systems in which the presence of O_2 is inconsequential. This field is still in its infancy, nonetheless the reported O_2-tolerant systems present innovative routes to efficient, aerobic proton reduction. Broadly speaking the current examples fall into one of three areas of catalyst: proton reducing enzymes (hydrogenases),[14] molecular complexes[5] and catalytic surfaces.[15,16]

In this perspective, each of these examples will be discussed to encourage a holistic development of O_2-tolerant catalyst systems. A discussion of the electrochemical/spectroscopic study of O_2-tolerance is also provided to highlight key techniques that will be vital for fully understanding the effects of O_2 on a proton reduction system.

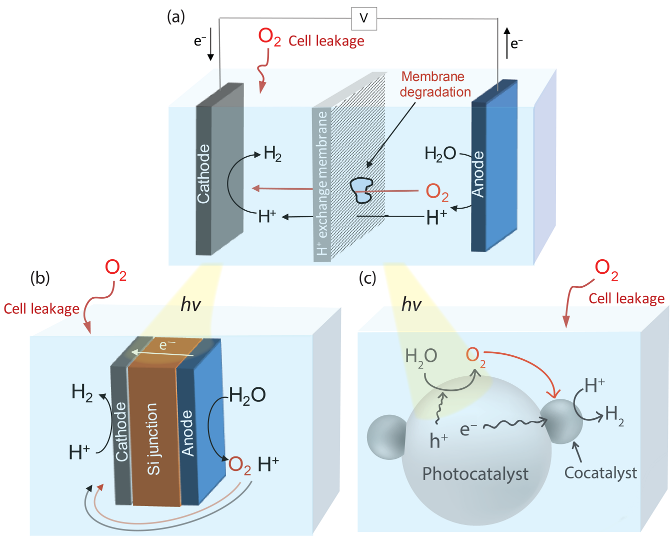

Figure 1. Potential routes through which a proton reducing catalyst could be exposed to O_2 in (a) a standard electrolysis/PEC cell, (b) an artificial leaf and (c) photocatalytic water-splitting particles.

2. Oxygen in a proton reducing system

Proton reduction is a pH dependent redox process that has a formal redox potential, $E^{0\prime}$, of 0 – (pH × 59) mV *vs.* NHE (25 °C). Applied potentials below $E^{0\prime}$ are needed to drive H_2 evolution and under aerobic conditions it is necessary to consider the effect such potentials have on O_2. In a pH 7 solution there are a number of potential O_2 reduction reactions that could occur, many of which form reactive oxygen species (ROS):[17]

Water formation:

$O_2 + 4H^+ + 4e^- \rightarrow 2H_2O$ $\quad {}^7E^{0\prime} = +0.82$ V (2)

ROS formation:

$O_2 + 2H^+ + 2e^- \rightarrow H_2O_2$ $\quad {}^7E^{0\prime} = +0.28$ V (3)

$O_2 + e^- \rightarrow O_2^-$ $\quad {}^7E^{0\prime} = -0.33$ V (4)

$H_2O_2 + H^+ + e^- \rightarrow HO\cdot + H_2O$ $\quad {}^7E^{0\prime} = +0.38$ V (5)

ROS reduction

$H_2O_2 + 2H^+ + 2e^- \rightarrow 2H_2O$ $\quad {}^7E^{0\prime} = +1.35$ V (6)

$HO\cdot + H^+ + e^- \rightarrow H_2O$ $\quad {}^7E^{0\prime} = +2.32$ V (7)

$O_2^- + 2H^+ + e^- \rightarrow H_2O_2$ $\quad {}^7E^{0\prime} = +0.89$ V (8)

Proton reduction:

$2H^+ + 2e^- \rightarrow H_2$ $\quad {}^7E^{0\prime} = -0.41$ V (9)

Potentials stated vs. NHE

Direct O_2 reduction to water through reaction (2) forms the most thermodynamically stable product, but the process is kinetically slow due to the dissociation energy of the dioxygen bond,[18] which has a considerable thermodynamic barrier of 498 kJ mol^{-1}. The reduction also requires 4 e$^-$ and 4 H$^+$ and therefore, with the exception of a few highly active catalytic sites, it is much more likely that incomplete O_2 reduction occurs to form H_2O_2, O_2^- or ·OH if sufficiently reducing conditions are available [reactions (3) to (5)]. These species can subsequently be reduced to water in a multi-step reaction sequence [reactions (6) to (8)].

Each of the O_2-reduction reactions (2) to (8) occurs at a less negative potential than the proton reduction reaction (9), which implies that any system capable of reducing protons will have sufficient driving force for O_2 reduction to either generate water or ROS. It should be noted that photochemical systems may also generate reactive singlet O_2 ($^1O_2$) through triplet-triplet annihilation. The interaction of a H_2 evolving catalyst with O_2 has two potential outcomes: O_2-tolerant proton reduction or inhibited catalysis due to O_2-sensitivity (Figure 2).

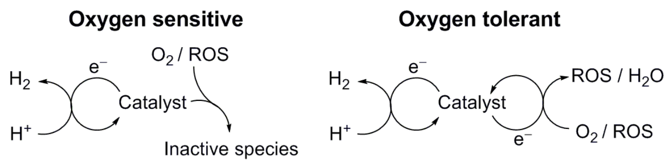

Figure 2. Two routes through which O_2 can affect catalytic proton reduction.

Oxygen-sensitive catalyst

O_2-sensitive proton reduction catalysts undergo a critical drop in H_2 production activity in the presence of O_2. In this case the catalyst is susceptible to deactivation by reaction with O_2 or with the ROS produced in reactions (3), (4), (5) or (8). The reducing sites at which O_2 or ROS attack are typically essential to proton reduction activity and therefore the catalyst is irreversibly inhibited.

O_2-sensitive catalysts require a defensive approach to overcome irreversible O_2 inhibition (see below). This involves protecting a catalyst from exposure to O_2/ROS in order to generate a locally anaerobic environment.

Oxygen-tolerant catalyst

O_2-tolerance is a term used to describe a catalyst that maintains a degree of activity in the presence of O_2. In this case the catalyst is able to reduce the incoming O_2 or ROS without being irreversibly damaged. Proton reduction is therefore in competition with O_2 reduction and H_2 is produced at a decreased rate and efficiency under aerobic conditions.

The reduction of O_2 by O_2-tolerant catalysts can be seen as an offensive approach to prevent O_2-inhibition. The catalyst is able to remove O_2 as a threat and allows H_2 evolution to continue. Designing a proton reduction catalyst capable of reducing O_2 and ROS to harmless by-products is an elegant strategy to realise aerobic proton reduction. O_2-tolerance can be enhanced further through design of a catalyst that has favourable kinetics for proton reduction over O_2 reduction.

3. Analytical techniques to study oxygen tolerance

Studying the O_2 tolerance of a proton reducing species is a relatively new line of research and as such, routine analytical techniques are not commonplace in most laboratories. Currently, electrochemistry offers the simplest and most effective approach. Analysis of currents stemming from a catalyst and quantification of the H_2 produced can be used to calculate turnover frequencies (TOFs),[19] turnover numbers (TONs) and determine redox processes under O_2.[20] These techniques can be applied across all types of hydrogen-evolving catalysts.

Cyclic voltammetry (CV) offers a fast method to study redox changes and catalytic currents. CV analysis starts from a catalytically-inert potential and scans to a more negative potential at which clear proton reduction currents are observable. The onset of proton reduction and size of the reduction wave, along with Tafel slope analysis, provide a measure of a catalyst's activity. The first step in the study of O_2 tolerance is to establish whether this activity changes under aerobic conditions. If a catalyst is O_2 sensitive, a CV in air will result in a significant drop in proton reduction current, whereas little change in the proton reduction wave indicates O_2-tolerant catalysis. An O_2-tolerant catalyst may also display an O_2 reduction wave, demonstrating simultaneous proton/O_2 reduction. O_2 tolerance is visible on a Pt electrode, where an O_2 reduction wave (onset +0.5 V *vs.* NHE) can be observed under an O_2 atmosphere, whilst the proton reduction wave (onset around −0.4 V) is maintained (Figure 3). CV only gives an indication of O_2-tolerance on a short time-scale, and analysis must therefore be supplemented with other techniques.

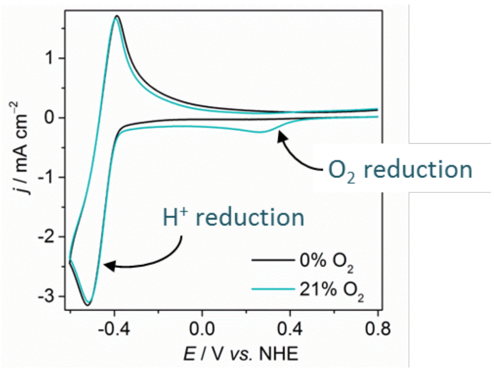

Figure 3. Cyclic voltammograms on a Pt disk electrode in phosphate buffer (pH 7, 0.1 M) under aerobic and anaerobic conditions at a scan rate of 50 mV s^{-1} at room temperature.[21]

Controlled potential electrolysis (CPE) is another vital tool in the study of proton reduction catalysis. In this process a constant potential is applied to a catalyst, allowing measurable quantities of H_2 to build up that can be quantified through techniques such as gas chromatography. Confirming that H_2 has been produced under aerobic conditions is of paramount importance, as otherwise it is not clear if an observed current stems from H_2 evolution or O_2/ROS reduction. Quantification of H_2 also allows the Faradaic efficiency (FE) to be calculated. FE is a measure of the electrons used *vs.* the H_2 produced and would be 100% if all electrons were consumed for proton reduction. Quantification of the H_2 produced and FE from CPE under aerobic and anaerobic atmospheres gives a clear indication of a catalyst's O_2 tolerance and selectivity for proton reduction over O_2 reduction. CPE is also necessary to establish long-term catalytic stability under O_2, as inhibition may occur over prolonged O_2/ROS exposure. Such experiments may be further extended to include the effect of varying levels of O_2 on catalysis.

Interaction between photocatalysts and O_2 may also be studied using surface photovoltage spectroscopy. This technique monitors the contact potential difference as a function of photon energy in order to determine the surface states and energy necessary for O_2 reduction on a given substrate.[22]

At present, analysis of O_2-tolerance is confined to measuring the H_2 produced by a catalyst with and without O_2, however this should be coupled with analysis of the formed ROS to gain a complete appreciation of the catalyst's aerobic activity. Rotating ring-disk electrochemistry is one of the most common methods of ROS detection, which can distinguish the production of H_2O_2 *vs.* H_2O. This technique requires a disk electrode, consisting of the catalyst to be studied, encircled by an electrode ring, which is typically Pt. When this electrode is rotated there is laminar flow of solution from the central disk to the outer ring electrode.[20] By holding the ring at oxidizing potentials with a bipotentiostat, it is possible to detect products from O_2 and H^+ reduction through their unique redox potentials. This technique can be used to monitor the production of H_2O_2 or H_2,[23] which can determine the degree of selectivity and O_2-tolerance of a given proton reduction catalyst.[24]

A range of electrochemical sensors can similarly be implemented to detect the formation of ROS. Detection of O_2^- has been achieved by a number of protein-based electrodes, such as those loaded with superoxide dismutase[25–27] or cytochrome c[28,29] and more recently, protein-free detectors have been utilised.[30–32] Similarly H_2O_2 can be detected through attachment of horseradish peroxidase,[33] cytochrome c[34] or CuS[35] to an electrode. This subject has recently been reviewed.[36]

ROS detection can also be achieved through the measurement of a unique spectroscopic signal, such as the distinct UV/vis peak of H_2O_2[37] and mass-spectrometry allows the quantification of $^{18}O_2$ reduction to $H_2{}^{18}O$. Alternatively, spectroscopic probes can be used, which can specifically determine nM concentrations of a given ROS.[38] Spectroscopic probing of the catalyst during proton reduction is equally important in order to visualise the structural changes that lead to O_2-sensitivity and tolerance. Through such analysis a complete appreciation for ROS/H_2 formed at a given applied potential *vs.* current expended can be realised, allowing conclusions concerning the interaction of the catalyst with O_2 to be drawn.

4. Oxygen-tolerant hydrogenases

Hydrogenases are nature's H_2-cycling catalysts and display a high 'per active site' activity with TOFs up to 10^4 s^{-1}, rivalling that of Pt.[39,40] These enzymes consist of well-suited structures to undertake proton reduction/H_2 oxidation and as such have received much attention.[14] [NiFe] and [FeFe] hydrogenases, categorised according to their active site composition, are the two classes of hydrogenases capable of proton reduction to H_2. In each hydrogenase the active metal ions are ligated by CN^-, CO and cysteine ligands and are typically connected to the protein exterior *via* iron-sulphur clusters. The disadvantages to the use of hydrogenases include difficult and costly purification, fragility, a large catalyst footprint (high 'volume per active site' ratio) and an infamous sensitivity to small quantities of O_2.

Hydrogenase interaction with O_2 is a considerably well-established area of research and may be instrumental in engineering O_2-tolerant synthetic systems.[41] In-depth electrochemical and spectroscopic studies have illustrated the route to O_2 inhibition across a range of hydrogenases and this work has been reviewed a number of times.[14,42] As such this perspective will only briefly summarise the interaction between hydrogenases and O_2 and instead focus on emerging strategies to shield the enzyme from aerobic atmospheres.

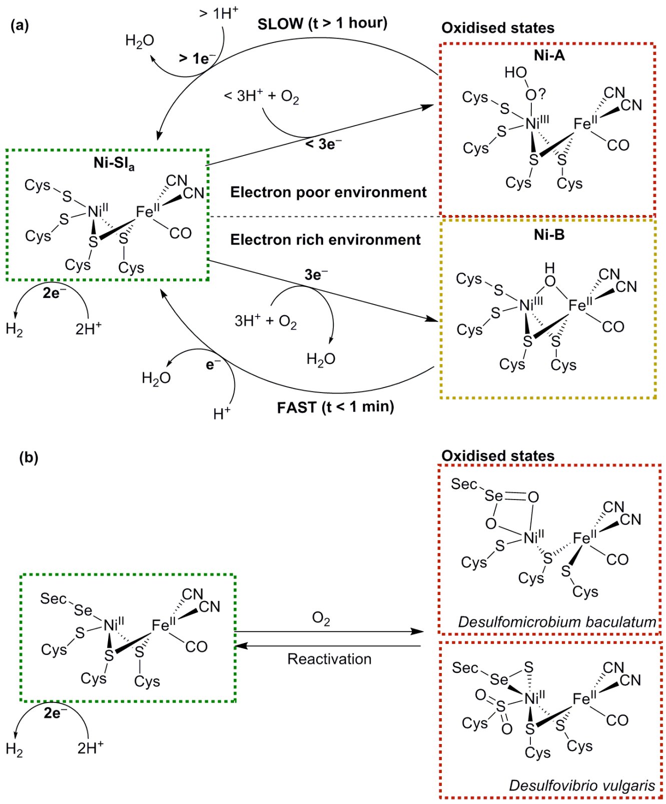

Figure 4. (a) Schematic representation of the formation and recovery of the oxidised Ni-A and Ni-B states in the [NiFe] hydrogenase active site (adapted from ref 43). (b) Active site of the [NiFeSe] hydrogenase and two reported oxidised structures from *Desulfomicrobium baculatum* (Ox4B state) *and Desulfovibrio vulgaris* (conformer I).

Both classes of hydrogenase consist of a range of subclasses and the O_2 susceptibility of each depends to some extent on the environment in which the enzyme functions biologically. Generally, both the [NiFe] and [FeFe] hydrogenases are inhibited by O_2 due to their interaction with ROS. Upon exposure of a [FeFe] hydrogenase to air, the active site, known as the H-cluster, is believed to form a ROS, which oxidises its proximal [4Fe-4S] cluster and prevents electron transfer through the enzyme to the active site.[44] [NiFe] hydrogenases deactivate through the reduction of O_2 to form an oxidised and paramagnetic 'unready' Ni-A state of the active site that is slow to reactivate[45] (see Figure 4a). The exact form of this state is debated, but crystallographic studies have suggested that a hydroperoxo ligand is ligated to the Ni ion as a result of incomplete O_2 reduction.[46]

The concept of O_2-tolerant H_2 oxidation has become an exciting branch of research, in particular for the membrane-bound [NiFe] hydrogenase from *Ralstonia eutropha,* which can oxidise H_2 under atmospheric levels of O_2.[47–49] O_2-tolerant hydrogenases are more likely to form a paramagnetic Ni-B (or 'ready') state upon exposure to O_2, as a result of more complete O_2 reduction to form a bridging hydroxo ligand.[46] The route to their tolerance is believed to originate from six cysteine residues surrounding the unique proximal [4Fe-3S] cluster next to the enzyme's active site.[50] The cysteines facilitate structural changes that allow the cluster to transfer two electrons within a small potential range.[51,52] When O_2 enters the active site, one electron from the reduced Ni^{II} and two from the proximal [4Fe-3S] cluster allow the hydrogenase to consistently form the Ni-B state (Figure 4a), which very quickly reactivates (t < 1 min). Recent evidence has suggested that conversion from Ni-A to Ni-B is also assisted by the oxygenation of one of the bridging S-atoms.[53] Despite promising O_2-tolerance, this exceptional type of [NiFe] hydrogenase is biased towards H_2 oxidation over proton reduction and is inhibited by H_2.[42]

The [NiFeSe] hydrogenase is a subclass of the [NiFe] hydrogenase that is highly active for proton reduction in the presence of H_2 and illustrates a promising degree of tolerance to O_2.[14] [NiFeSe] hydrogenases contain a ligated selenocysteine moiety in place of one of the terminal cysteines of the conventional [NiFe] enzyme (Figure 4). O_2 exposure of the enzyme does not form substantial quantities of Ni-A/Ni-B states and a paramagnetic Ni^{III} is not observed.[54] The major products from oxidation of two [NiFeSe] hydrogenases are presented in Figure 4b. The active site from *Desulfomicrobium baculatum* when crystallised aerobically contains an oxidised selenocysteine moiety (referred to as Ox4B)[54] and the *Desulfovibrio vulgaris* species, when purified and crystallised aerobically, contains an oxidised Se and doubly-oxidised S (referred to as conformer I).[55,56] The chemical role of selenocysteine in protecting the hydrogenase from oxidative damage is currently under investigation,[57] but it has been shown that the [NiFeSe] hydrogenase is able to reactivate faster under anaerobic conditions after O_2-exposure in comparison to the O_2-sensitive [NiFe] species.[58] The O_2 tolerance may be a result of the easier oxidation and reduction of Se compared to S.[59]

Due to the extreme O_2 sensitivity of many hydrogenases, engineering the enzymes to reduce protons and O_2 simultaneously is a significant challenge,[60,61] and currently

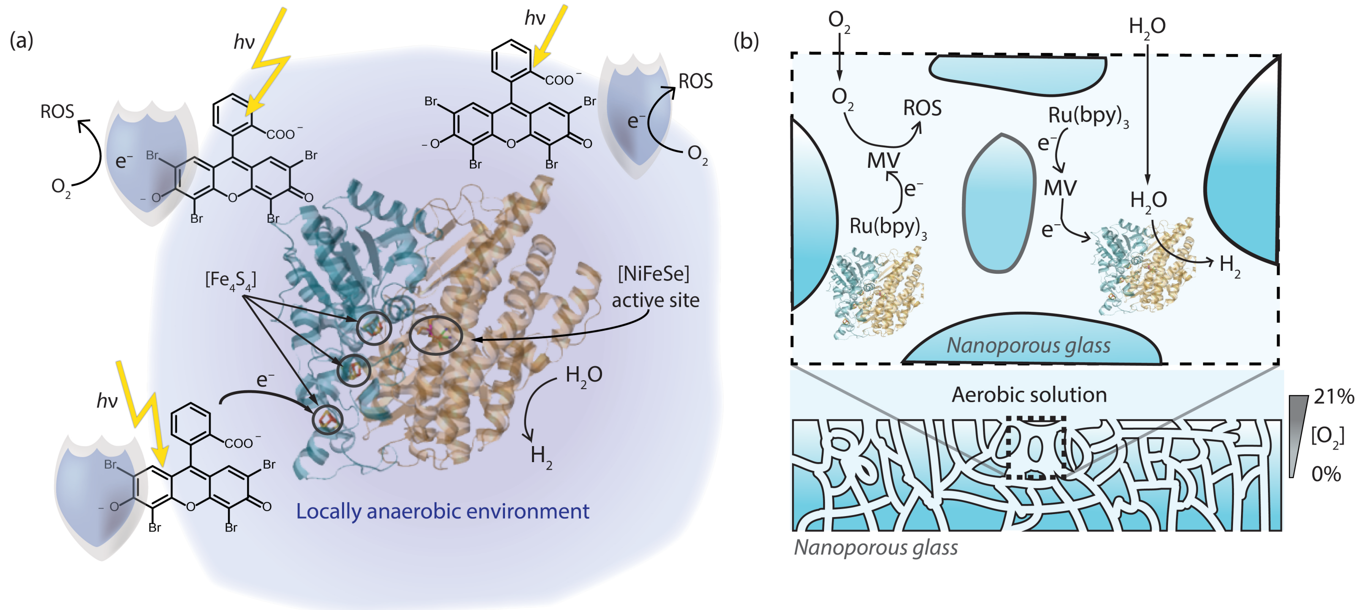

Figure 5. (a). Photo-excited eosin Y as a shield to protect a [NiFeSe] hydrogenase.[62] (b) O_2-shielding strategy based on a multi-component system consisting of a Ru dye, methyl viologen as soluble redox mediator and a hydrogenase in nanoporous glass. Reduced methyl viologen is generated upon photo-excitation of the dye and used to reduce the hydrogenase and quench O_2 inside the pores to produce an anaerobic environment.[63] The sacrificial electron donor used to quench the dye omitted for clarity in (a) and (b).

more practicable approaches to aerobic H_2-evolution involve shielding the enzyme from exposure to O_2. This involves a 'retrofitted' O_2-defending shield that reduces O_2 before it can have adverse effects on enzyme activity. To date, 'shields' have been predominantly based on photochemical systems that remove O_2 from a system during irradiation.

In 2009 we reported that *D. baculatum* [NiFeSe] hydrogenase attached to a Ru-sensitised TiO_2 nanoparticle was able to produce H_2 photocatalytically in a N_2 purged vial outside a glovebox.[64] Although this sacrificial photosystem sustains H_2 generation under traces of O_2, it cannot maintain photo-H_2 production activity under atmospheric O_2 levels due to the lack of efficient O_2 shielding and presumably enzyme-damaging ROS formation on TiO_2 in the presence of O_2 (see section 5).

Peters and coworkers showed in 2012 that a [NiFe] hydrogenase from *Thiocapsa roseopersicina* covalently linked to a Ru dye was able to photocatalytically reduce protons under aerobic conditions in the presence of the soluble redox mediator methyl viologen (MV) and a sacrificial electron donor.[65] Under an aerobic atmosphere and an initial lag period where dissolved O_2 was photo-reduced, this system generated H_2 at 11% of the initial rate observed under pseudo-inert conditions. An analogous system that used a Ru dye, which was not linked to the enzyme, showed no activity under air. It was therefore concluded that by attaching the Ru dye to the hydrogenase a local concentration of reduced MV was generated around the hydrogenase, which reduced O_2 before it reached the enzyme and partially shielded it from inhibition.

Another example of O_2-shielding came in 2013,[62] when we reported photocatalytic H_2 production with a *D. baculatum* [NiFeSe] hydrogenase and the organic dye eosin Y in the presence of a sacrificial electron donor (Figure 5a). The photoactivity of this mediator-free system was tested under increasing concentrations of O_2 and it was able to maintain a notable degree of photocatalytic activity. Even under 21% O_2, 10% of the enzyme's activity (corresponding to a TOF of 1.5 s^{-1}) was sustained relative to the anaerobic experiment, without the observation of a significant lag phase to start H_2 production. Excited eosin Y promotes proton reduction and conversion of O_2 to $^1O_2$.[66] The O_2-tolerance of the system may therefore stem from the fast formation of $^1O_2$ by the dye, which presumably reacts with eosin Y or the electron donor to create an anaerobic environment (Figure 5a).

The concept of shielding has been extended by Dewa and coworkers through the implementation of porous enzyme-immobilising frameworks.[63] In this case, a nanoporous glass plate was soaked in a tris(bipyridine)ruthenium^{II} dye, MV and a [NiFe] hydrogenase from *Desulfovibrio vulgaris*. The nanoporous framework consisted of 50 nm channels that directed diffusion of O_2 into the structure. The MV reduced O_2 in the channels as it entered the glass during irradiation, producing a shielded pathway that allowed protons to reach the hydrogenase but not O_2 (Figure 5b). The glass framework thereby allowed sacrificial H_2 evolution to be powered photocatalytically through the Ru dye. The system was able to generate H_2 at photocatalytic rates as high as 7.9 s^{-1} per enzyme, with a TON of 130,000 over 12 hours under aerobic atmospheres.

Shielding strategies have also been applied to H_2 oxidising systems. Redox active polymers containing viologen moieties are capable of simultaneously immobilising and protecting hydrogenases during H_2 oxidation,[67,68] and 3D porous carbon electrodes loaded with hydrogenase have sustained H_2 oxidation activity by favouring the effusion of H_2 over O_2.[69] These approaches could also be employed for H_2 evolving systems.

Despite being complex and multifaceted, the interaction between hydrogenses and O_2 is generally thoroughly investigated. Yet there is currently enormous scope for the development of improved O_2 shielding systems and scaffolds to protect the enzyme to allow the use of more O_2-sensitive hydrogenases in less stringent environments. Future work should remove redox mediators and sacrificial agents from these systems and focus on constructing O_2 shields on hydrogenase-modified electrodes to retroactively produce O_2-tolerant hydrogenase systems.

5. Oxygen-tolerant molecular synthetic catalysts

Synthetic molecular catalysts are discrete transition metal complexes consisting of metal/ligand combinations designed to promote proton reduction.[70,4] Study of their activity is normally restricted to the homogeneous phase, containing the dissolved catalyst and an electron source, which is typically an electrode, a dye with a sacrificial electron donor or a strong chemical reducing agent. Recent examples have shown innovative rational design[71–75] and the field has been reviewed numerous times.[5,76] These catalysts do not typically exhibit TONs or TOFs comparable to hydrogenases, but offer a defined catalytic site that can be used to establish functionality and mechanisms that are essential for efficient proton reduction activity.

Molecular catalysts are often inspired by the active site of hydrogenase enzymes and are frequently referred to as 'artificial hydrogenases' accordingly.[77] Due to the low tolerance of hydrogenases towards O_2, for a long time molecular catalysts were assumed to be unusable under aerobic conditions,[5] however it is becoming increasingly apparent that molecular synthetic catalysts do not necessarily exhibit the debilitating O_2-sensitivity of the enzymes they mimic.

Our group reported the first full study of O_2-tolerant proton reduction with a synthetic molecular complex.[78] The study used a water-soluble $[Et_3NH][Co^{III}Cl(dimethylglyoximato)_2(pyridyl\text{-}4\text{-}hydrophosphonate)]$ catalyst (Figure 6 shows fully protonated complex **1A**) and explored changes in activity under varying levels of O_2. CVs of the catalyst were undertaken under N_2, O_2 and CO (Figure 7).[79] Catalytic currents were seen under N_2 and O_2 (Figure 7a) but not CO, a known catalytic inhibitor (Figure 7b). The large difference in proton reduction current between the CO-inhibited CV and the aerobic CV illustrates the O_2-tolerant activity of the complex. Evidence of O_2 reduction was also visible as the non-catalytic Co^{II}/Co^{III} oxidation wave from the cobaloxime was not seen under aerobic conditions and the size of the Co^{III}/Co^{II} wave increased, indicating competitive O_2 reduction by the cobaloxime in the Co^{II} oxidation state (Figure 7a).

Subsequent CPE of this complex under inert and aerobic conditions at $E_{appl} = -0.7$ V *vs.* NHE showed that substantial H_2 production activity remained in the presence of O_2. After re-purging the aerobic catalyst solution with N_2 and repeating CPE, the cobaloxime regained 100% of its initial activity, suggesting the drop in activity under air was a result of competitive O_2 reduction by the cobaloxime and not O_2 sensitivity.

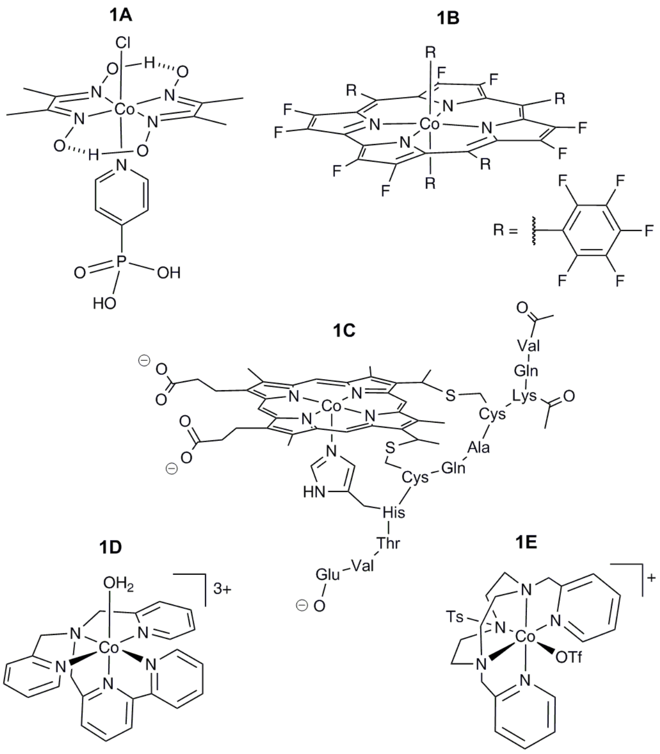

Figure 6. Currently known Co-based O_2-tolerant molecular proton reduction catalysts. **1A:** Water-soluble cobaloxime;[78] **1B**: Fluorinated Co corrole;[80] **1C:** Acetylated Co microperoxidase-11;[81] **1D/1E**: Co polypyridyl catalysts.[82,83]

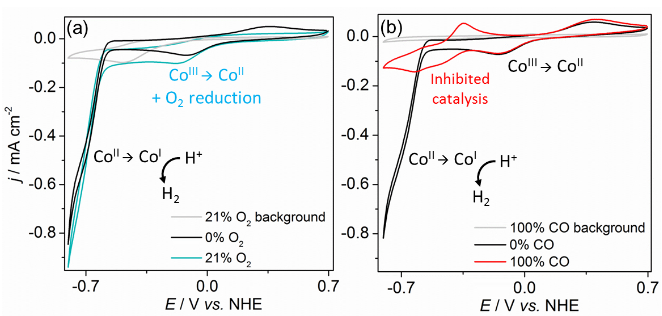

Figure 7. CVs of **1A** (1mM) in 0.1 M TEOA/Na_2SO_4 at pH 7 under atmospheres of (a) N_2 and air and (b) N_2 and CO. Scan rate was 100 mV/s on a glassy carbon working electrode. Taken from reference 79.

Photochemical experiments supported this result. Catalysis was driven photochemically using either a heterogeneous Ru-photosensitised TiO_2 nanoparticle system or a homogeneous dye, eosin Y, and the evolved H_2 was measured under increasing concentrations of O_2. Under 21% O_2, 70% of the original H_2 evolution activity was measured in the homogenous system and 17% was maintained in the colloidal system, which illustrated the O_2 tolerance of the cobaloxime complex.

Subsequent experiments with other cobaloxime variants have shown similar levels of O_2 tolerance.[24,84]

It should be noted that the degree of O_2 tolerance exhibited by **1A** varied depending on the electron source and as such the dye or electrode and corresponding applied potential to the catalyst must be considered when studying molecular systems under O_2. Most commonly used electrodes are capable of reducing O_2 to some extent and any currents stemming from a homogeneous catalyst must be deconvoluted from this background electrode activity. CVs of glassy carbon in air show a wave at −0.5 V *vs.* NHE in pH 7 solution (Figure 7a, background) and FEs will typically be significantly less than the expected 100% for the same reason.[79] The photosensitiser will also react with O_2 during catalysis, lowering the rate of electron transfer to the catalyst and producing ROS. Organic dyes, such as fluorescein, rose bengal and eosin Y are common photosensitisers due to their appealing lack of precious metal centre, however under O_2 they are a source of $^1O_2$,[66] which will rapidly react with catalyst ligands. Ruthenium polypyridine dyes are similarly quenched by O_2.[85] These dyes can be coupled to TiO_2 to assist in charge separation, however the TiO_2 is capable of producing ROS in the form of O_2^- and OOH^- during irradiation.[86] The low activity of the heterogeneous TiO_2-based system that drove photocatalysis of **1A** could be a result of O_2^- formation with concomitant desorption or decomposition of the Ru dye or catalyst.[87]

Following on from the cobaloxime system, a Co corrole catalyst synthesized by the Dey group demonstrated similar levels of O_2 tolerance (**1B**, Figure 6).[80] The study used a fluorinated macrocycle to decrease the overpotential needed for proton reduction and catalytic activity was established using a rotating ring-disk electrode consisting of the complex immobilised on an edge plane graphitic electrode with a Pt ring. Rotating ring-disk experiments were carried out in the presence of O_2, allowing the authors to analyse the O_2 reduction by the Co corrole through oxidation of the generated H_2O_2. This demonstrated the real time reduction of protons to H_2 under aerobic conditions by the catalyst and CPE gave a FE of 52% under air after 10 hours of electrolysis in 0.5 M H_2SO_4. The O_2 tolerance of the Co corrole stems from its ability to reduce O_2 without deactivation, which has been reported previously.[88]

Bren and coworkers demonstrated that an acetylated Co microperoxidase-11 complex (**1C**, Figure 6) was O_2 tolerant.[81] This catalyst has a macrocyclic centre similar to that of **1B** and showed a high FE of 85% when CPE was carried out over 4 hours in a pH 7 solution (13% lower than the equivalent experiment under N_2). The high FE seen in this case may be a result of the large applied overpotential (850 mV), making the barrier of proton reduction over O_2 reduction less significant. In such a case the relative concentrations of protons over O_2 would determine catalyst selectivity. At room temperature the concentration of O_2 is 0.3 mM under aerobic conditions[89] with a diffusion coefficient of $2\cdot10^{-5}$ cm^2 s^{-1},[90] and is therefore outmatched by the highly available and fast diffusing protons.

Cobalt polypyridyl catalysts have also demonstrated a degree of tolerance to O_2. These catalysts typically show high stability towards deactivation and a number of structural variants have been synthesized.[91,92] [Co(N,N-bis(2-pyridinylmethyl)-2,2'-bipyridine-6-methanamine)(OH_2)][PF_6]$_3$ ([Co(DPA-Bpy)(H_2O)][PF_6]$_3$) (**1D**, Figure 6) is an O_2-tolerant Co polypyridyl complex published by Zhao and coworkers.[82] Using a $[Ru(bpy)_3]^{2+}$ photosensitiser in the presence of ascorbic acid as a sacrificial electron donor, the catalyst retained 40% of its activity in the presence of air, however this was not explored in more detail. This has been followed up by Lloret-Fillol and coworkers who used a 4-di(picolyl)7-(p-toluenesulfonyl)-1,4,7-triazacyclononane (Py_2^{TS}tacn) ligand to form a Co complex capable of generating H_2 under O_2 (**1E**, Figure 6).[83] In this case 25% of catalytic activity was maintained under air using a molecular Ir photosensitiser.

The O_2-tolerant catalysts discussed thus far have a similar structure, consisting of N-ligating ligands to a Co centre. Proton reduction in such species is thought to occur through Co^{II}/Co^{I} intermediates to form a Co^{III}–H.[93,94,82] The hydridic intermediate may then reduce a proton to form H_2 or be further reduced to Co^{II}–H, which evolves H_2 (Figure 8). Each of the reduced Co centres could also be active for O_2 reduction[95,96] (Figure 8) and there is precedent for the formation of H_2O_2 by cobaloximes[24,97] and H_2O by Co corroles.[88] Proficient reduction of O_2 and ROS to harmless species by these catalysts may explain their limited deactivation in a similar manner to O_2-tolerant hydrogenases. The catalytic core of these complexes is also comparable to Vitamin B12 and parallels can be drawn between the H_2 production and O_2 reduction activity of these species.[96] Comparison of these complexes to biological structures will be useful in understanding the effects of O_2 inhibition in both classes of catalyst.

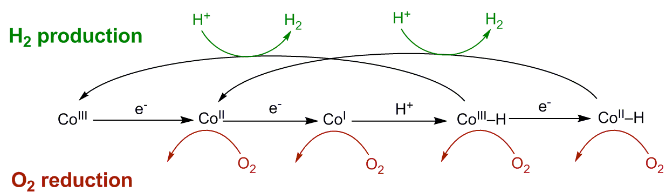

Figure 8. The proposed mechanism for heterolytic H_2 evolution from Co complexes **1A-E** and the potential O_2 reduction reactions that could be carried out at the reduced intermediates. Adapted from a Figure in reference 98.

It is important for the study of O_2-tolerant molecular complexes to move away from the Co-N based scaffold and branch out into different ligand structures and metal centres to establish other functionalities insensitive to deactivation. A recent study of O_2 tolerance with a Ni bis(diphosphine) catalyst (**1F**, Figure 9) was consequently carried out by our group.[79] The cyclic phosphine ligand-set coordinated to Ni contains pendant amines, which serve as proton relays that has led to TOFs comparable to hydrogenases.[72,75] CV of this catalyst showed little difference between anaerobic and aerobic conditions, however CPE at −0.4 V *vs.* NHE at pH 4.5 produced 1.05 µmol of H_2 (72% FE) under N_2, but no H_2 under 21% O_2, indicating a high degree of O_2-sensitivity.[79] In its native Ni^{2+} oxidation state this catalyst is air stable, suggesting that a reduced form of the catalyst is susceptible to reaction with ROS/O_2. The inactivation has been assigned to oxidation of the phosphine ligands to phosphine oxides during turnover under O_2 (Figure 9), which show no proton reduction activity. This effect has been observed when using similar structures as O_2 reduction catalysts.[99]

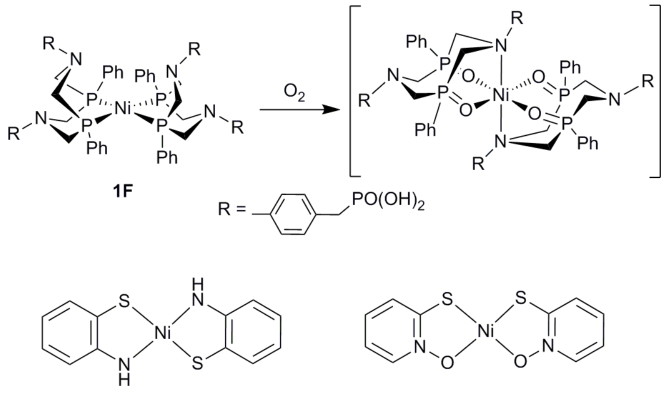

Figure 9. The O_2-sensitive Ni bis(diphospine) complex, **1F**, and the proposed route of inhibition. Complexes **1G** and **1H** are O_2 tolerant square planar Ni complexes.[100]

Recently two square planar Ni thiolate-containing complexes have shown a more promising degree of O_2 tolerance. These simple structures are notable for their high stability and in a recent report Eisenberg and coworkers showed that catalysts **1G** and **1H** (Figure 9) exhibited TONs of 62,000 and 80,000, respectively, over 40 h CPE in aerobic solutions.[100] CV of the catalysts was reportedly identical under Ar or air and CPE showed a 15-18% drop in FE between aerobic and inert conditions (80 to 98% for **1G** and 78 to 93% for **1H**). The high FE suggests that these catalysts are particularly robust in air, which may be related to the high overpotential applied (between 700-800 mV), much like catalyst **1C**.

To gauge the current state of O_2-tolerant molecular proton reduction catalysts, all known examples and their catalytic properties are summarised in Tables 1 and 2. In an ideal situation, H_2 would be produced at mild overpotentials, with the same rate and efficiency regardless of whether O_2 is present. This is not yet the case, however, examples continue to push the boundaries of what was previously thought possible and it appears that this could be realised within the next few years.

There are many other known molecular catalysts that should be studied under O_2 to establish a clear trend between catalyst structure and O_2-tolerant proton reduction. It is also important that O_2-tolerance studies are carried out in aqueous solution, rather than commonly used organic solvents as the solubility and behaviour of O_2 in these environments is drastically different ([O_2] in acetonitrile = 8.1 mM at 25 °C).[101] Computational studies have begun to establish the effects of O_2 on a molecular catalyst structure,[102] but further expansion and comparison to experimental data is required. Future investigation must also include the study of ROS intermediates and their interaction with metal complexes to establish the O_2 reduction tendencies of the O_2-tolerant *vs.* the O_2-sensitive catalysts. Nevertheless, at present it would seem that choosing a molecular catalyst capable of both catalytic O_2 and proton reduction is the most viable strategy to attain an O_2-tolerant molecular system.

6. Oxygen-tolerant catalytic surfaces

'Catalytic surfaces' is a broad term that we apply to heterogeneous surfaces, nanoparticles and immobilised assemblies in this perspective. Given their generally high stability and amenability to widespread use, such surfaces have been able to produce large amounts of H_2 at rates rivalling those of enzymatic systems and many new examples have recently emerged.[15,103] The wide scope for structural and geometric modification through methods such as doping, nanostructuring or controlled deposition of multifunctional layers has allowed rational surface design to maximise catalytic turnover and stability.[12,104,105] Their use includes a few disadvantages however, as they have generally low 'per atom activity' and ascertaining the exact nature of the catalytically active site and mechanism can be difficult.

Table 1. Summary of O_2-tolerant molecular electrocatalysts and their H_2 production activity under O_2.

Complex	Catalyst / electrode material	TOF under anaerobic/ aerobic atm. (h^{-1})	pH	Over-potential	FE under anaerobic/ aerobic atm.	Ref.
1A	Cobaloxime / glassy carbon	3.68 / 0.83	7	290 mV	67 / 10 to 43%	78,79
1B	Co corrole / graphite	N/A	0	800 mV	N/A / 52%	80
1C	Acetylated Co microperoxidase-11 / Hg pool	6250 / 4750	7	850 mV	98 / 85%	81
1G	[Ni(2-aminobenzenethiolate)$_2$] / glassy carbon	N/A / 1550	7	800 mV	93 / 78%	100
1H	[Ni(2-pyridinethiolate-N-oxide)$_2$] / glassy carbon	N/A / 2000	7	780 mV	98 / 80%	100

Table 2. Summary of photocatalytic systems with O_2-tolerant molecular catalysts and their H_2 production activity under O_2.

Complex	Catalyst/ photosensitiser	TOF under anaerobic/ aerobic atm. (h^{-1})	% Activity in aerobic atm.	pH	λ of light	Ref.
1A	Cobaloxime / TiO_2-tris(bipyridine)Ru	15 / 2.6	17%	7	λ > 420 nm	78
1A	Cobaloxime / eosin Y	62.5 / 44.2	70%	7	λ > 420 nm	78
1D	$[Co(DPA\text{-}Bpy)(H_2O)][PF_6]_3$ / tris(bipyridine)Ru	N/A	40%	4	450 nm	82
1E	$[Co(CF_3SO_3)(Py_2{}^{TS}tacn)][CF_3SO_3]$ / bis(2-phenylpyridine)(bipyridine)Ir	147 / 44	30%	N/A	447 nm	83

Heterogeneous surfaces are considerably less sensitive to O_2 than molecular complexes and hydrogenases (presumably due to the absence of fragile organic ligand frameworks) and many proton reducing surfaces are active O_2 reduction catalysts.[106,107] New developments in this field are instead focused on increasing catalytic selectivity for H_2 evolution over O_2 reduction in order to maximise efficiency.

Surface engineering to exclude O_2 diffusion to the active catalyst seeks to defend catalytic surfaces from O_2 entirely. One example of O_2 exclusion has been presented by Domen and coworkers on a photocatalytic water-splitting particle consisting of a $(Ga_{1-x}Zn_x)(N_{1-x}O_x)$ photocatalyst loaded with Rh. O_2 is particularly problematic in these systems as the Rh is able to catalyse the H_2 and O_2-consuming back reaction of water splitting (the reverse of reaction 1).[13] It was found that the back reaction could be completely prevented through the use of a Cr_2O_3 layer. When the Rh cocatalyst was coated with Cr_2O_3 the water-splitting activity was greatly enhanced as the Cr_2O_3 blocked O_2 from diffusing to the Rh surface (Figure 10a).[108,109] This effect was confirmed through a voltammetric study of a Cr_2O_3-coated Rh electrode, which showed complete loss of the O_2 reduction wave on Rh.[110] Proton reduction activity still remained and was only slightly diminished as a result of the Cr_2O_3 layer blocking some catalytic sites on the Rh. This was confirmed through infrared spectroscopy, which illustrated that protons were able to penetrate the Cr_2O_3 to reach a catalytic Pt surface.

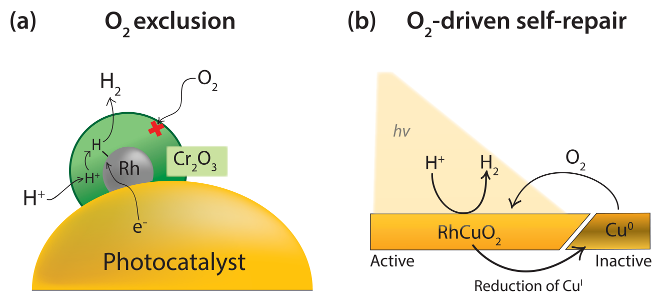

Figure 10. (a) Schematic representation of O_2 exclusion by a Cr_2O_3 layer loaded on a Rh cocatalyst for photocatalytic water splitting.[110] (b) Illustration of O_2-driven self-repair after photocorrosion of a $CuRhO_2$ electrode to form inactive Cu^0.[111]

A similar strategy has been utilised by Dey and coworkers using ammonium tetrathiomolybdate (ATM),[112] a reagent commonly used as a precursor to hydrogen-evolving MoS_x. It was proposed that the ATM formed a layer on Au that could shuttle protons, whilst preventing access of O_2 to catalytically active sites. CV of an ATM-Au electrode showed no O_2 reduction wave and CPE with 180 mV applied overpotential under air gave a high FE of 89% for proton reduction over 10 hours. The oxygen tolerance of the MoS_x archetype is believed to originate from the S ligand, which plays a key role in the proton reduction mechanism.[103]

A number of other surface coatings have been able to prevent O_2 reduction at photocatalyst surfaces, such as: lanthanoid oxide layers based on La, Pr, Sm, Gd, and Dy on Rh loaded $(Ga_{1-x}Zn_x)(N_{1-x}O_x)$;[113] amorphous Si and Ti oxyhydroxides on perovskite-type oxynitride, $LaMg_xTa_{1-x}O_{1+3x}N_{2-3x}$ ($x \geq 1/3$);[114] surface-corroded Ti^{4+}-doped Fe_2O_3;[115] electrodeposited amorphous TiO_2 on W-doped $BiVO_4$;[116] NiO-loaded on $NaTaO_3$[117] and cocatalysts of Au or RuO_2.[12,118] O_2-excluding SiO_2 layers for electrocatalytic CO_2 reduction have also emerged[119] and the presence of Li^+ counter ions over K^+ or Na^+ has been shown to assist in the preclusion of O_2 reduction.[120]

Other strategies to prevent a catalyst from O_2 interaction may be achievable through O_2-impermeable polymers. Research in this field is well-established due to its amenability to industrial applications, such as O_2-impermeable packaging materials. A number of polymer layers are generally impermeable to O_2 and thin coatings of metal oxides such as ZnO/ SiO_x and Al can lower the O_2 permeability further.[121]

Preventing O_2 reduction can also be achieved through use of selective catalysts. Takanabe and coworkers have synthesised tungsten carbide nanoparticle cocatalysts that illustrate an affinity for proton reduction over O_2 reduction catalysis.[122] Loading the nanoparticles onto a Na-doped $SrTiO_2$ photocatalyst increased H_2-evolution activity and prevented O_2 reduction, which led to the UV light-driven production of stoichiometric quantities of H_2 and O_2 through water splitting.

Alternatively, O_2 in solution can be used to maintain a catalytic structure through O_2-driven self-repair. This has been demonstrated by Bocarsly and coworkers using a delafossite $CuRhO_2$ structured electrode that functions most effectively under 100% O_2 (Figure 10b).[111] O_2-driven self-repair is a form of O_2 tolerance that reduces O_2 to regenerate the active catalytic material. $CuRhO_2$ is a photocathode for proton reduction at an applied bias of −0.7 V *vs.* NHE in 1 M NaOH. Under inert atmospheres the surface is active for 3 hours of photoelectrolysis, whereas in an O_2 atmosphere the activity remained constant over 8 hours. The increased stability in the presence of O_2 was proven via X-ray photoelectron spectroscopy to be a result of regeneration of Cu^I by dissolved O_2, which precluded the formation of Cu^0 deposits on the surface. The material had a lowered FE compared to surfaces under inert atmospheres, at 80%, however this number is respectable in such challenging conditions and the lost efficiency is merely a result of the O_2 reduction necessary for electrode regeneration.

In a similar example to the delafossite electrode above, a $CuFeO_2$ electrode presented by Choi and coworkers was more stable in the presence of O_2.[123] The surface was able to produce H_2 under visible light with an applied bias of –1.4 V *vs.* NHE in O_2-saturated 1 M NaOH. The electrode had a photon to current ratio of 2.2% under Ar saturated and 3.7% under O_2 saturated solutions suggesting that the electrode was less selective towards H_2 evolution than $CuRhO_2$. This has since been followed up by the Sivula group who described a sol-gel technique to fabricate a similar electrode,[124] which was further doped with O_2 to improve catalyst stability. O_2-driven 'self-repair' offers a promising route to O_2 tolerant proton reduction, however all delafossite structures discussed require atmospheres of 100% O_2 to function most effectively, which complicates their use under atmospheric conditions.

Heterogeneous, proton-reducing surfaces offer the most simple and robust strategies to achieve O_2-tolerant H_2 evolution. The use of O_2-excluding layers is particularly interesting as the approach is also amenable to the systems discussed in sections 4 and 5 of this perspective. It should be noted that it is still rare for H_2 evolution activity to be studied under aerobic conditions and future study of the presented strategies under higher levels of O_2 is therefore necessary.

7. Conclusion and future outlook

This perspective describes the state-of-the-art for the rapidly developing field of O_2-tolerant proton reduction catalysis. Each of the catalytic classes discussed in sections 4 to 6 demonstrate distinct approaches to achieve aerobic proton reduction, which revolve around either a defensive or an offensive strategy (Figure 11). Future advances will surely involve a combined use of such techniques across enzymatic, molecular and surface-based catalysts, which we hope to bring together in this work.

Defensive methods to preclude O_2 inhibition will allow the use of O_2-sensitive catalysts under less stringent conditions. The use of O_2 shields offers a simple and effective approach to remove O_2, but such systems do not ensure complete elimination of O_2 from a system and greatly lower catalytic efficiency. O_2-exclusion layers are in theory a more effective route for O_2-sensitive systems as they generate an effectively anaerobic environment for catalysis. These would be particularly useful for highly O_2-sensitive catalysts, such as hydrogenases.

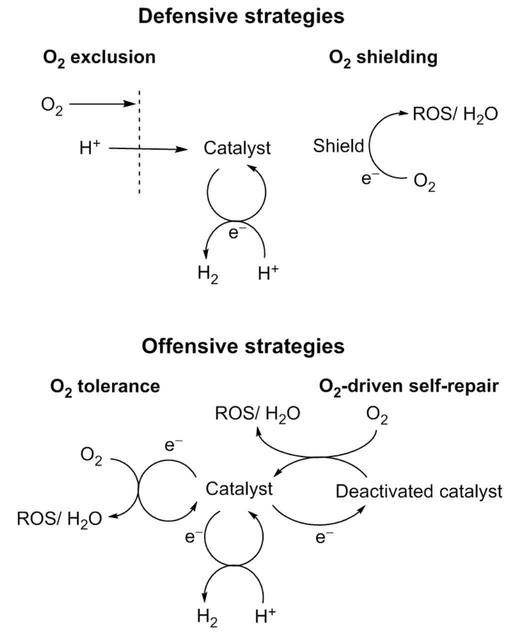

Figure 11. A summary of the offensive/defensive strategies used to evolve H_2 in the presence of O_2.

Offensive techniques utilise the catalytic centre to remove O_2 from solution without damaging the catalyst and will be much simpler to utilise on a large scale. O_2 tolerance has been identified in a number of catalysts and although not formally tested, is presumably present in a number of other species. O_2 tolerance results in a lowered efficiency for proton reduction and decreasing the catalytic affinity for O_2 reduction is therefore the predominant issue to be solved. O_2-tolerant systems can be further optimised through combination with defensive strategies, such as O_2-exclusion layers. Alternatively O_2 can be used to improve the stability of reductively corroded catalysts through O_2-driven self-repair, taking advantage of oxidising aerobic atmospheres. This has proven particularly useful for delafossite structured catalysts and may also prove effective for other catalysts that decompose in inert atmospheres.

To make further progress in this field it is important that O_2 inhibition becomes a more common test of a proton reduction system. A tolerance to O_2 is an excellent trait for a catalyst to exhibit and should be reported alongside other catalytic properties. Establishing the impact of O_2 is simple; a catalyst's interaction with O_2 can be studied with an extra electrolysis or photolysis experiment under aerobic conditions rather than an inert atmosphere.

More in depth studies of O_2-tolerant catalyst systems should also become commonplace. Future studies would benefit from the use of rotating ring-disk electrodes and quantification of the produced ROS to help gain a better understanding of catalytic behaviour and deactivation pathways under air. Appreciating the factors that contribute to proton reduction inhibition by O_2 should then pave the way for water splitting systems capable of functioning flawlessly under aerobic conditions. Whether such a system would be best implemented with an enzymatic, molecular or surface-based catalyst is yet to be determined, however the chemical strategies used to avoid O_2 inhibition can mutually benefit the field as a whole.

The strategies considered in this perspective are also applicable to the production of other renewable fuels. Catalytic processes, such as CO_2 reduction, offer alternate routes to artificial photosynthesis and would similarly benefit from O_2-tolerant catalysts (for high aerobic stability) in combination with O_2-exclusion strategies (for high efficiency). There are also other inhibitors to investigate, such as CO, which is formed in synthesis gas producing systems or through unwanted side reactions (e.g. in formic acid decomposition), the impact of which is seldom explored.[79] Understanding inhibition across a range of inhibitors and catalytic processes will have the dual benefit of increasing our understanding of catalytic active sites and increasing the viability of each system to more widespread production of sustainable, pollution-free fuel.

Acknowledgements

Financial support from the EPSRC (EP/H00338X/2), the Christian Doppler Research Association (Austrian Federal Ministry of Science, Research and Economy and National Foundation for Research, Technology and Development), and the OMV Group is gratefully acknowledged. Further thanks are extended to Mr. Timothy E. Rosser, Dr. Chong-Yong Lee and Dr. Hyun S. Park for useful comments and fruitful discussions.

Notes and references

[a]Christian Doppler Laboratory for Sustainable SynGas Chemistry, Department of Chemistry, University of Cambridge, Lensfield Road, Cambridge CB2 1EW, U.K.; E-mail: reisner@ch.cam.ac.uk; Homepage: http://www-reisner.ch.cam.ac.uk/.

Electronic Supplementary Information (ESI) gives the data used to prepare Figure 3. See DOI: 10.1039/x0xx00000x

DOI: 10.1039/c000000x/

1. J. Barber, *Chem. Soc. Rev.*, 2009, **38**, 185–196.
2. Y. Tachibana, L. Vayssieres, and J. R. Durrant, *Nat. Photonics*, 2012, **6**, 511–518.
3. C.-Y. Lin, D. Mersch, D. A. Jefferson, and E. Reisner, *Chem. Sci.*, 2014, **5**, 4906–4913.
4. V. S. Thoi, Y. Sun, J. R. Long, and C. J. Chang, *Chem. Soc. Rev.*, 2013, **42**, 2388–2400.
5. W. T. Eckenhoff and R. Eisenberg, *Dalton Trans.*, 2012, **41**, 13004–13021.
6. F. E. Osterloh, *J. Phys. Chem. Lett.*, 2014, **5**, 2510–2511.
7. C.-Y. Lin, Y.-H. Lai, D. Mersch, and E. Reisner, *Chem. Sci.*, 2012, **3**, 3482–3487.
8. L. Ghassemzadeh, K.-D. Kreuer, J. Maier, and K. Müller, *J. Phys. Chem. C*, 2010, **114**, 14635–14645.
9. M. Danilczuk, F. D. Coms, and S. Schlick, *J. Phys. Chem. B*, 2009, **113**, 8031–8042.
10. D. G. Nocera, *Acc. Chem. Res.*, 2012, **45**, 767–776.
11. R. E. Rocheleau, E. L. Miller, and A. Misra, *Energy & Fuels*, 1998, **12**, 3–10.
12. A. Kudo and Y. Miseki, *Chem. Soc. Rev.*, 2009, **38**, 253–278.
13. K. Maeda and K. Domen, *J. Phys. Chem. Lett.*, 2010, **1**, 2655–2661.
14. W. Lubitz, H. Ogata, O. Rüdiger, and E. Reijerse, *Chem. Rev.*, 2014, **114**, 4081–4148.
15. P. C. K. Vesborg, B. Seger, and I. Chorkendorff, *J. Phys. Chem. Lett.*, 2015, **6**, 951–957.
16. C. C. L. McCrory, S. Jung, I. M. Ferrer, S. M. Chatman, J. C. Peters, and T. F. Jaramillo, *J. Am. Chem. Soc.*, 2015, **137**, 4347–4357.
17. P. M. Wood, *Biochem. J.*, 1988, **253**, 287–289.
18. A. A. Gewirth and M. S. Thorum, *Inorg. Chem.*, 2010, **49**, 3557–3566.
19. C. Costentin, S. Drouet, M. Robert, and J.-M. Savéant, *J. Am. Chem. Soc.*, 2012, **134**, 11235–11242.
20. A. J. Bard and L. R. Faulkner, *Electrochemical Methods: Fundamentals and Applications*, Wiley, New York, 2nd edn., 2001.
21. *Electrochemical measurements were carried out on a potentiostat (Ivium) with a Ag/AgCl reference electrode (sat. KCl, BASi) and a platinum-mesh counter electrode. Potentials were converted to NHE through the relationship: 0 V vs. NHE = 0.197 V vs. Ag/AgCl.*
22. J. Zhao and F. E. Osterloh, *J. Phys. Chem. Lett.*, 2014, **5**, 782–786.
23. E. Yeager, *Electrochim. Acta*, 1984, **29**, 1527–1537.
24. N. Kaeffer, A. Morozan, and V. Artero, *J. Phys. Chem. B*, 2015, DOI: 10.1021/acs.jpcb.5b03136.
25. Y. Tian, L. Mao, T. Okajima, and T. Ohsaka, *Anal. Chem.*, 2002, **74**, 2428–2434.
26. L. Campanella, G. Favero, and M. Tomassetti, *Anal. Lett.*, 1999, **32**, 2559–2581.
27. M. I. Song, F. F. Bier, and F. W. Scheller, *Bioelectroch. Bioener.*, 1995, **38**, 419–422.
28. K. Tammeveski, T. T. Tenno, A. A. Mashirin, E. W. Hillhouse, P. Manning, and C. J. McNeil, *Free Radical Biol. Med.*, 1998, **25**, 973–978.
29. W. Scheller, W. Jin, E. Ehrentreich-Förster, B. Ge, F. Lisdat, R. Büttemeier, U. Wollenberger, and F. W. Scheller, *Electroanalysis*, 1999, **11**, 703–706.
30. H. Flamm, J. Kieninger, A. Weltin, and G. A. Urban, *Biosens. Bioelectron.*, 2015, **65**, 354–359.
31. X. J. Chen, A. C. West, D. M. Cropek, and S. Banta, *Anal. Chem.*, 2008, **80**, 9622–9629.
32. S. Madhurantakam, S. Selvaraj, N. Nesakumar, S. Sethuraman, J. B. B. Rayappan, and U. M. Krishnan, *Biosens. Bioelectron.*, 2014, **59**, 134–139.
33. Q. Zhang, Y. Qiao, L. Zhang, S. Wu, H. Zhou, J. Xu, and X.-M. Song, *Electroanalysis*, 2011, **23**, 900–906.
34. C. Xiang, Y. Zou, L.-X. Sun, and F. Xu, *Electrochem. Commun.*, 2008, **10**, 38–41.
35. J. Bai and X. Jiang, *Anal. Chem.*, 2013, **85**, 8095–8101.
36. C. Calas-Blanchard, G. Catanante, and T. Noguer, *Electroanalysis*, 2014, **26**, 1277–1286.

37. J. M. Burns, W. J. Cooper, J. L. Ferry, D. W. King, B. P. DiMento, K. McNeill, C. J. Miller, W. L. Miller, B. M. Peake, S. A. Rusak, A. L. Rose, and T. D. Waite, *Aquat. Sci.*, 2012, **74**, 683–734.
38. G. Bartosz, *Clin. Chim. Acta*, 2006, **368**, 53–76.
39. P. M. Vignais and B. Billoud, *Chem. Rev.*, 2007, **107**, 4206–4272.
40. A. K. Jones, E. Sillery, S. P. J. Albracht, and F. A. Armstrong, *Chem. Commun.*, 2002, 866–867.
41. M.-E. Pandelia, H. Ogata, and W. Lubitz, *ChemPhysChem*, 2010, **11**, 1127–1140.
42. B. Friedrich, J. Fritsch, and O. Lenz, *Curr. Opin. Biotechnol.*, 2011, **22**, 358–364.
43. F. A. Armstrong, N. A. Belsey, J. A. Cracknell, G. Goldet, A. Parkin, E. Reisner, K. A. Vincent, and A. F. Wait, *Chem. Soc. Rev.*, 2009, **38**, 36–51.
44. S. T. Stripp, G. Goldet, C. Brandmayr, O. Sanganas, K. A. Vincent, M. Haumann, F. A. Armstrong, and T. Happe, *Proc. Natl. Acad. Sci. U.S.A.*, 2009, **106**, 17331–17336.
45. H. Ogata, S. Hirota, A. Nakahara, H. Komori, N. Shibata, T. Kato, K. Kano, and Y. Higuchi, *Structure*, 2005, **13**, 1635–1642.
46. A. Volbeda, L. Martin, C. Cavazza, M. Matho, B. W. Faber, W. Roseboom, S. P. J. Albracht, E. Garcin, M. Rousset, and J. C. Fontecilla-Camps, *J. Biol. Inorg. Chem.*, 2005, **10**, 239–249.
47. L. Lauterbach and O. Lenz, *J. Am. Chem. Soc.*, 2013, **135**, 17897–17905.
48. T. Burgdorf, O. Lenz, T. Buhrke, E. van der Linden, A. K. Jones, S. P. J. Albracht, and B. Friedrich, *J. Mol. Microbiol. Biotechnol.*, 2005, **10**, 181–196.
49. G. Goldet, A. F. Wait, J. A. Cracknell, K. A. Vincent, M. Ludwig, O. Lenz, B. Friedrich, and F. A. Armstrong, *J. Am. Chem. Soc.*, 2008, **130**, 11106–11113.
50. J. Fritsch, P. Scheerer, S. Frielingsdorf, S. Kroschinsky, B. Friedrich, O. Lenz, and C. M. T. Spahn, *Nature*, 2011, **479**, 249–252.
51. A. Volbeda, P. Amara, C. Darnault, J.-M. Mouesca, A. Parkin, M. M. Roessler, F. A. Armstrong, and J. C. Fontecilla-Camps, *Proc. Natl. Acad. Sci. U.S.A.*, 2012, **109** , 5305–5310.
52. Y. Shomura, K.-S. Yoon, H. Nishihara, and Y. Higuchi, *Nature*, 2011, **479**, 253–256.
53. M. Horch, L. Lauterbach, M. A. Mroginski, P. Hildebrandt, O. Lenz, and I. Zebger, *J. Am. Chem. Soc.*, 2015, **137**, 2555–2564.
54. A. Volbeda, P. Amara, M. Iannello, A. L. De Lacey, C. Cavazza, and J. C. Fontecilla-Camps, *Chem. Commun.*, 2013, **49**, 7061–7063.
55. M. C. Marques, R. Coelho, I. A. C. Pereira, and P. M. Matias, *Int. J. Hydrogen Energy*, 2013, **38**, 8664–8682.
56. M. C. Marques, R. Coelho, A. L. De Lacey, I. A. C. Pereira, and P. M. Matias, *J. Mol. Biol.*, 2010, **396**, 893–907.
57. C. Wombwell and E. Reisner, *Chem. Eur. J.*, 2015, **21**, 8096–8104.
58. M. Teixeira, G. Fauque, I. Moura, P. A. Lespinat, Y. Berlier, B. Prickril, H. D. Peck Jr., A. V. Xavier, J. Le Gall, and J. J. G. Moura, *Eur. J. Biochem.*, 1987, **167**, 47–58.
59. O. Skaff, D. I. Pattison, P. E. Morgan, R. Bachana, V. K. Jain, K. I. Priyadarsini, and M. J. Davies, *Biochem. J.*, 2012, **441**, 305–316.
60. V. Radu, S. Frielingsdorf, S. D. Evans, O. Lenz, and L. J. C. Jeuken, *J. Am. Chem. Soc.*, 2014, **136**, 8512–8515.
61. S. V. Hexter, F. Grey, T. Happe, V. Climent, and F. A. Armstrong, *Proc. Natl. Acad. Sci. U.S.A.*, 2012, **109**, 11516–11521.
62. T. Sakai, D. Mersch, and E. Reisner, *Angew. Chem. Int. Ed.*, 2013, **52**, 12313–12316.
63. T. Noji, M. Kondo, T. Jin, T. Yazawa, H. Osuka, Y. Higuchi, M. Nango, S. Itoh, and T. Dewa, *J. Phys. Chem. Lett.*, 2014, **5**, 2402–2407.
64. E. Reisner, D. J. Powell, C. Cavazza, J. C. Fontecilla-Camps, and F. A. Armstrong, *J. Am. Chem. Soc.*, 2009, **131**, 18457–18466.
65. O. A. Zadvornyy, J. E. Lucon, R. Gerlach, N. A. Zorin, T. Douglas, T. E. Elgren, and J. W. Peters, *J. Inorg. Biochem.*, 2012, **106**, 151–155.
66. A. P. Gerola, J. Semensato, D. S. Pellosi, V. R. Batistela, B. R. Rabello, N. Hioka, and W. Caetano, *J. Photochem. Photobiol. A.*, 2012, **232**, 14–21.
67. S. V. Morozov, O. G. Voronin, E. E. Karyakina, N. A. Zorin, S. Cosnier, and A. A. Karyakin, *Electrochem. Commun.*, 2006, **8**, 851–854.
68. N. Plumeré, O. Rüdiger, A. A. Oughli, R. Williams, J. Vivekananthan, S. Pöller, W. Schuhmann, and W. Lubitz, *Nat. Chem.*, 2014, **6**, 822–827.
69. L. Xu and F. A. Armstrong, *RSC Adv.*, 2015, **5**, 3649–3656.
70. C. Tard and C. J. Pickett, *Chem. Rev.*, 2009, **109**, 2245–2274.
71. H. I. Karunadasa, E. Montalvo, Y. Sun, M. Majda, J. R. Long, and C. J. Chang, *Science*, 2012, **335**, 698–702.
72. M. L. Helm, M. P. Stewart, R. M. Bullock, M. Rakowski DuBois, and D. L. DuBois, *Science*, 2011, **333**, 863–866.
73. W. R. McNamara, Z. Han, P. J. Alperin, W. W. Brennessel, P. L. Holland, and R. Eisenberg, *J. Am. Chem. Soc.*, 2011, **133**, 15368–15371.
74. Z. Han, W. R. McNamara, M.-S. Eum, P. L. Holland, and R. Eisenberg, *Angew. Chem. Int. Ed.*, 2012, **51**, 1667–1670.
75. M. A. Gross, A. Reynal, J. R. Durrant, and E. Reisner, *J. Am. Chem. Soc.*, 2014, **136**, 356–366.
76. T. S. Teets and D. G. Nocera, *Chem. Commun.*, 2011, **47**, 9268–9274.
77. G. Caserta, S. Roy, M. Atta, V. Artero, and M. Fontecave, *Curr. Opin. Chem. Biol.*, 2015, **25**, 36–47.
78. F. Lakadamyali, M. Kato, N. M. Muresan, and E. Reisner, *Angew. Chem. Int. Ed.*, 2012, **51**, 9381–9384.
79. D. W. Wakerley, M. A. Gross, and E. Reisner, *Chem. Commun.*, 2014, **50**, 15995–15998.
80. B. Mondal, K. Sengupta, A. Rana, A. Mahammed, M. Botoshansky, S. G. Dey, Z. Gross, and A. Dey, *Inorg. Chem.*, 2013, **52**, 3381–3387.
81. J. G. Kleingardner, B. Kandemir, and K. L. Bren, *J. Am. Chem. Soc.*, 2014, **136**, 4–7.
82. W. M. Singh, T. Baine, S. Kudo, S. Tian, X. A. N. Ma, H. Zhou, N. J. DeYonker, T. C. Pham, J. C. Bollinger, D. L. Baker, B. Yan, C. E. Webster, and X. Zhao, *Angew. Chem. Int. Ed.*, 2012, **51**, 5941–5944.
83. A. Call, Z. Codolà, F. Acuña-Parés, and J. Lloret-Fillol, *Chem. Eur. J.*, 2014, **20**, 6171–6183.
84. D. W. Wakerley and E. Reisner, *Phys. Chem. Chem. Phys.*, 2014, **16**, 5739–5746.
85. S. Ji, W. Wu, W. Wu, P. Song, K. Han, Z. Wang, S. Liu, H. Guo, and J. Zhao, *J. Mater. Chem.*, 2010, **20**, 1953–1963.
86. Y.-F. Li and A. Selloni, *J. Am. Chem. Soc.*, 2013, **135**, 9195–9199.

87. K. Hanson, M. K. Brennaman, H. Luo, C. R. K. Glasson, J. J. Concepcion, W. Song, and T. J. Meyer, *ACS Appl. Mater. Interfaces*, 2012, **4**, 1462–1469.
88. A. Schechter, M. Stanevsky, A. Mahammed, and Z. Gross, *Inorg. Chem.*, 2012, **51**, 22–24.
89. R. Sander, *Atmos. Chem. Phys. Discuss.*, 2014, **14**, 29615–30521.
90. P. Han and D. M. Bartels, *J. Phys. Chem.*, 1996, **100**, 5597–5602.
91. Y. Sun, J. P. Bigi, N. A. Piro, M. L. Tang, J. R. Long, and C. J. Chang, *J. Am. Chem. Soc.*, 2011, **133**, 9212–9215.
92. R. S. Khnayzer, V. S. Thoi, M. Nippe, A. E. King, J. W. Jurss, K. A. El Roz, J. R. Long, C. J. Chang, and F. N. Castellano, *Energy Environ. Sci.*, 2014, **7**, 1477–1488.
93. M. Razavet, V. Artero, and M. Fontecave, *Inorg. Chem.*, 2005, **44**, 4786–4795.
94. R. M. Kellett and T. G. Spiro, *Inorg. Chem.*, 1985, **24**, 2373–2377.
95. G. N. Schrauzer and L. P. Lee, *J. Am. Chem. Soc.*, 1970, **92**, 1551–1557.
96. G. N. Schrauzer, *Angew. Chem. Int. Ed. Engl.*, 1976, **15**, 417–426.
97. M. Shamsipur, A. Salimi, H. Haddadzadeh, and M. F. Mousavi, *J. Electroanal. Chem.*, 2001, **517**, 37–44.
98. J. L. Dempsey, B. S. Brunschwig, J. R. Winkler, and H. B. Gray, *Acc. Chem. Res.*, 2009, **42**, 1995–2004.
99. J. Y. Yang, R. M. Bullock, W. G. Dougherty, W. S. Kassel, B. Twamley, D. L. DuBois, and M. Rakowski DuBois, *Dalton Trans.*, 2010, **39**, 3001–3010.
100. A. Das, Z. Han, W. W. Brennessel, P. L. Holland, and R. Eisenberg, *ACS Catal.*, 2015, **5**, 1397–1406.
101. J. M. Achord and C. L. Hussey, *Anal. Chem.*, 1980, **52**, 601–602.
102. P. H.-L. Sit, R. Car, M. H. Cohen, and A. Selloni, *Proc. Natl. Acad. Sci. U.S.A.*, 2013, **110** , 2017–2022.
103. D. Merki and X. Hu, *Energy Environ. Sci.*, 2011, **4**, 3878–3888.
104. M. P. Soriaga, J. H. Baricuatro, K. D. Cummins, Y.-G. Kim, F. H. Saadi, G. Sun, C. C. L. McCrory, J. R. McKone, J. M. Velazquez, I. M. Ferrer, A. I. Carim, A. Javier, B. Chmielowiec, D. C. Lacy, J. M. Gregoire, J. Sanabria-Chinchilla, X. Amashukeli, W. J. Royea, B. S. Brunschwig, J. C. Hemminger, N. S. Lewis, and J. L. Stickney, *Surf. Sci.*, 2015, **631**, 285–294.
105. Y. Ma, X. Wang, Y. Jia, X. Chen, H. Han, and C. Li, *Chem. Rev.*, 2014, **114**, 9987–10043.
106. T. Wang, D. Gao, J. Zhuo, Z. Zhu, P. Papakonstantinou, Y. Li, and M. Li, *Chem. Eur. J.*, 2013, **19**, 11939–11948.
107. Y. Wang, E. Laborda, K. Tschulik, C. Damm, A. Molina, and R. G. Compton, *Nanoscale*, 2014, **6**, 11024–11030.
108. K. Maeda, K. Teramura, D. Lu, N. Saito, Y. Inoue, and K. Domen, *Angew. Chem. Int. Ed.*, 2006, **45**, 7806–7809.
109. K. Maeda, K. Teramura, D. Lu, N. Saito, Y. Inoue, and K. Domen, *J. Phys. Chem. C*, 2007, **111**, 7554–7560.
110. M. Yoshida, K. Takanabe, K. Maeda, A. Ishikawa, J. Kubota, Y. Sakata, Y. Ikezawa, and K. Domen, *J. Phys. Chem. C*, 2009, **113**, 10151–10157.
111. J. Gu, Y. Yan, J. W. Krizan, Q. D. Gibson, Z. M. Detweiler, R. J. Cava, and A. B. Bocarsly, *J. Am. Chem. Soc.*, 2014, **136**, 830–833.
112. S. Chatterjee, K. Sengupta, S. Dey, and A. Dey, *Inorg. Chem.*, 2013, **52**, 14168–14177.
113. M. Yoshida, K. Maeda, D. Lu, J. Kubota, and K. Domen, *J. Phys. Chem. C*, 2013, **117**, 14000–14006.
114. C. Pan, T. Takata, M. Nakabayashi, T. Matsumoto, N. Shibata, Y. Ikuhara, and K. Domen, *Angew. Chem. Int. Ed.*, 2015, **54**, 2955–2959.
115. D. Cao, W. Luo, J. Feng, X. Zhao, Z. Li, and Z. Zou, *Energy Environ. Sci.*, 2014, **7**, 752–759.
116. D. Eisenberg, H. S. Ahn, and A. J. Bard, *J. Am. Chem. Soc.*, 2014, **136**, 14011–14014.
117. Y. Matsumoto, U. Unal, N. Tanaka, A. Kudo, and H. Kato, *J. Solid State Chem.*, 2004, **177**, 4205–4212.
118. A. Iwase, H. Kato, and A. Kudo, *Catal. Lett.*, 2006, **108**, 7–10.
119. G. Yuan, A. Agiral, N. Pellet, W. Kim, and H. Frei, *Faraday Discuss.*, 2014, **176**, 233–249.
120. C. Ding, X. Zhou, J. Shi, P. Yan, Z. Wang, G. Liu, and C. Li, *J. Phys. Chem. B*, 2015, **119**, 3560–3566.
121. Y. Leterrier, *Prog. Mater. Sci.*, 2003, **48**, 1–55.
122. A. T. Garcia-Esparza, D. Cha, Y. Ou, J. Kubota, K. Domen, and K. Takanabe, *ChemSusChem*, 2013, **6**, 168–181.
123. C. G. Read, Y. Park, and K.-S. Choi, *J. Phys. Chem. Lett.*, 2012, **3**, 1872–1876.
124. M. S. Prévot, N. Guijarro, and K. Sivula, *ChemSusChem*, 2015, **8**, 1359–1367.

Table of Contents Artwork:

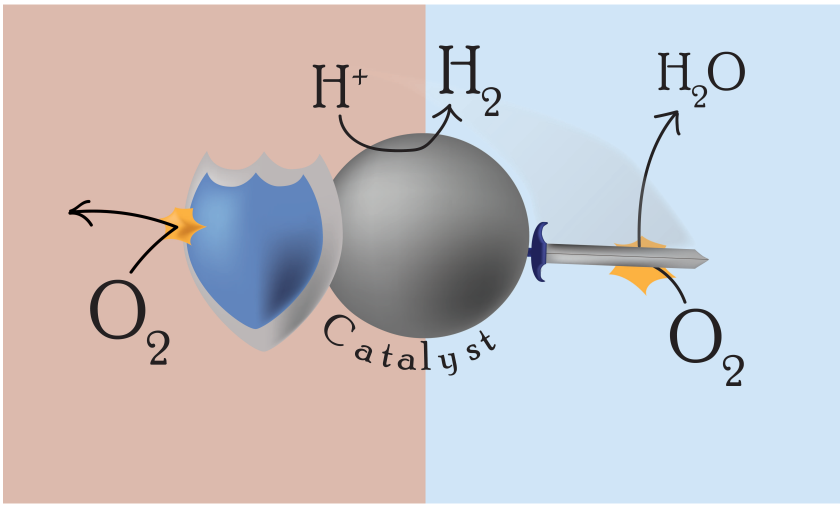

This perspective summarises strategies for avoiding adverse effects of O_2 on H_2-evolving enzymatic systems, molecular synthetic catalysts and catalytic surfaces.

Broader Context:

The generation of hydrogen from water is a potential approach to develop clean and renewable fuel. This process is carried out by proton reduction catalysts and currently research is focussed on the development of efficient and robust catalytic species. Application of the water-splitting process will be carried out on a large scale, not restricted to the laboratory, and as such it is necessary to consider how O_2 in our atmosphere or produced as a side product from water splitting would interact with such an arrangement. O_2 is an inhibitor of a number of catalytic processes and therefore designing strategies to avoid O_2 inhibition is crucial in the production of viable proton reduction systems.